

# Estimating Probability of Failure of Composite Laminated Panel with Multiple Potential Failure Modes

Chanyoung Park<sup>1</sup>, Nam H. Kim<sup>2</sup> and Raphael T. Haftka<sup>3</sup>  
*Department of Mechanical and Aerospace Engineering, University of Florida*  
*PO Box 116250, Gainesville, FL 32611-6250*

As composite structures play a key role in aircraft structure design, assessing probability of failure (PF) of the composite structures has become important to ensuring safety of the aircraft design. To assess the PF of the design, computational models are frequently used to estimate probability of the composite structures but the computational models have uncertainty in predicting failures due to lacking knowledge of composite structure failures. Structural tests can provide additional knowledge of the failures to effectively reduce the uncertainty in the computational model. The presence of multiple failure modes due to variabilities is the other concern because correlated failure modes causes difficulty to estimate PF and it brings significant error for use of the effective reliability analysis methods, such as FORM or SORM. Undetected failure mode is the other issue relevant to the multiple failure modes. A single test can detect one failure mode, each failure modes has different probability of occurrence. Hence, a existing failure mode may not be detected and neglected. Possibly we have significantly under estimated PF. In the study, we make an uncertainty quantification model to estimate PF for correlated failure modes. Also the probability of failure occurrence of each failure modes is also estimated with the model. The model is demonstrated through a simple example and PF estimation of a curved composite panel with a hole is made. From the numerical study, it is observed that performing a single failure test can significantly reduce conservativeness on estimating PF. Test for a given probability of failure allows lighter design.

## I. Introduction

ADVANCED composite materials have become key ingredients in modern aircraft structures due to their superior strength to weight ratio, stiffness tailorability, fatigue and corrosion properties. But composite structure design a disadvantage that use of the composite materials also induce large uncertainty in predicting failures with computational models, Uncertainty quantification becomes important for composite design to ensure its safety. Here, we make a model to quantify uncertainty in a composite fuselage panel design and predict probability of failure (PF) of panels based on the design. Two main features of the uncertainty model are that incorporating structural tests into the uncertainty model with error in the tests and considering multiple potential failure modes.

To incorporate test results into the computational model with its own uncertainty, we have to quantify uncertainty in the tests. But there is an obstacle to incorporate test result into the computational model. The computational model requires exact inputs parameters, such as material properties and dimensions, and predict output, such as buckling load, with uncertainty. To reduce the uncertainty in the outputs, tests also have to have negligible uncertainty in the inputs to properly incorporate test results into the computational model. However tests, particularly for composite structures, have large input uncertainty. Errors in measuring material properties are large while output uncertainties, such as errors in measuring strain and buckling load, are negligibly small (Ref. 2). To properly incorporate uncertainty in tests, uncertainty in inputs has to be converted to likelihood of output for given input.

Considering presence of multiple potential failure modes is another important issue for estimating probabilities of failure. Due to variability in manufacturing process, multiple failure modes may exist in a single design. The presence of failure mode switching can lead a undesirable situation. For example, buckling failure mode is dominant

---

<sup>1</sup> Graduate Research Assistant, AIAA Student Member.

<sup>2</sup> Associate Professor, AIAA Member.

<sup>3</sup> Distinguished Professor, AIAA Fellow.

at PF of  $10^{-2}$  level and strength failure mode is dominant at PF of  $10^{-4}$  then test can detect only buckling failure mode. Possibly the present of strength failure is neglected, we can significantly underestimate PF of design at low level PF. If we know the presence, it is hard to use the buckling test to reduce uncertainty in predicting the strength failure. Thus we need to estimate the possibility of failure mode switching and figure out a method to reduce uncertainty for both failure modes even with test results of only one failure modes.

Previous work (Ref. 5 and Ref. 6) quantified the effects of the structural tests on a structural design with simple design process with a single failure mode of structural strength using convolution integral to model uncertainty propagation and combination. In this study, we evaluate PF of cylindrical composite panels based on a design which was tested and analyzed by Knight and Starnes (Ref. 3) and Stanley (Ref. 4). Two correlated failure modes are considered as potential failure modes in the design. We use ABAQUS to predict failures and then the actual test result from their report will be used to reduce error in the failure prediction.

The objectives of this from ABAQUS study are as follows: i) present a methodology for a composite panel design to predict and include the effect of a test, ii) show the effects of structural test on reducing uncertainty in PF evaluation for a complex composite panel design, and iii) investigate the effects of the correlation on final PF evaluation is investigated.

The paper has three parts. Firstly, show uncertainty modeling to incorporate test results. Before estimating PF of the composite panel with the uncertainty model, PF estimation for a simple composite beam structure with two potential failure modes is made to validate the uncertainty model. Then finally we estimate PF for the composite panel model. We use non-linear analysis to predict buckling load and strength failure load.

## II. Evaluating Probability of Failure for a Composite Panel with a Hole

The composite panel was fabricated from commercially available unidirectional Thornel 300 graphite fiber tapes pre-impregnated with 450K cure Narmco 5208 thermosetting epoxy resin fixture (Ref. 3). The test specimen schematically shown in Fig. 1 is surrounded by a metallic test frame. The appropriate boundary conditions for the cylindrical panel are (i) fully clamped on the bottom edge, (ii) clamped except for axial motion on the top edge (potted end), and (iii) simply-supported on the vertical edges (knife-edge restraints). The test consists of statically imposing a uniform end-shortening,  $\delta$ , until the specimen reaches buckling point. Electrical strain gages were used to monitor surface strains near the hole in the axial direction. A single test was performed and buckling failure occurred and measured with the specimen.

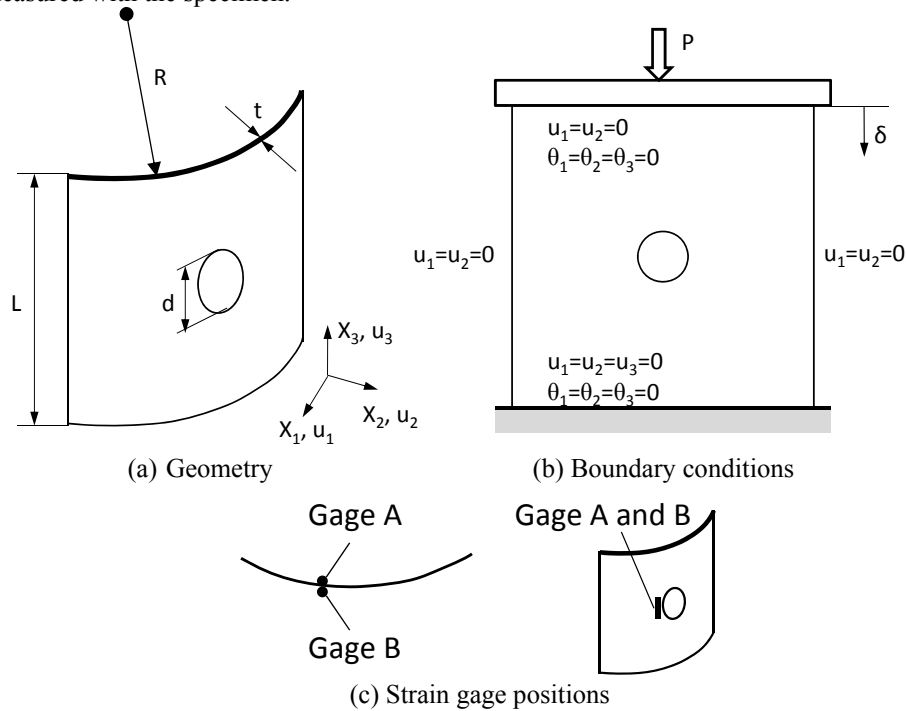


Figure 1. Magnetization as a function of applied field.

In this study, we assume that we have two potential modes, buckling failure and strength failure. The strength failure will be occurred by failure of a single sheet instead of progressive damage model. PF is defined as

$$Pf = \Pr(\hat{C}^\lambda < \hat{P} \text{ or } \hat{C}^s < \hat{P}) \quad (1)$$

where  $\hat{C}^\lambda$ ,  $\hat{C}^s$  and  $\hat{P}$  are random variables for modeling variabilities in capacity of buckling failure, capacity of strength failure, and external load, respectively.

### A. Modeling Uncertainty

For quantifying uncertainty of composite panels, two test stages in the building-block approach for structural tests shown in the Fig. 2 are considered. Design of a composite panel begins with coupon test ply material properties and their variability. The element test calibrate predicted performances of designs based on the measured material properties and their variability at coupon test level. In the paper, we recognize that composite panel is a structural element, and the buckling test is an element test.

To estimate PF, variability of capacity in the panels has to be quantified and computational models are needed to estimate the variability of capacity, such as buckling load, and PF corresponding to design allowable. However the computational model has error to predict the capacity, the error can lead significant error to predict the variability. Consequently we have large error in PF estimate.

When we include error in our estimation, the calculated buckling load distribution is widened and the widened distribution compensates the error in the calculation. We call the distribution as possible true distribution (PTD) which considering every possible uncertainties.

Figure 3 shows a process to obtain the PTD of buckling load. In uncertainty model, we have input uncertainties, such as variability in dimension  $f_{inp}(d)$  and in material property  $f_{inp}(m)$ . We then calculate the distribution of the buckling load  $f_{calc}(\lambda)$  based on the input parameters with a computational model. Finally the computational error is combined with the calculated capacity distribution,  $f_{calc}(\lambda)$  then the PTD of buckling load,  $f_{Prue}(\lambda)$ , is obtained.

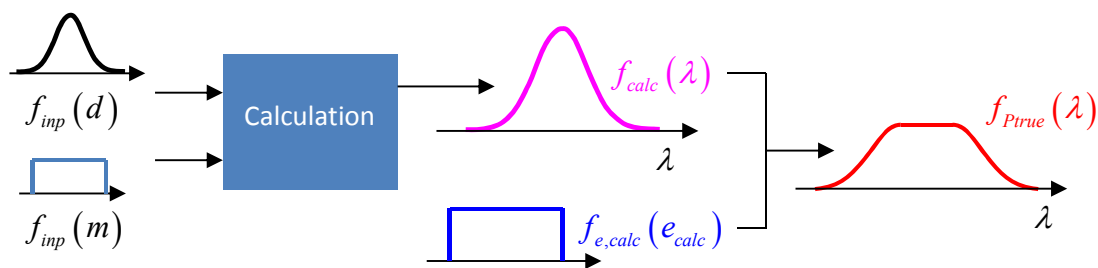


**Figure 3. Illustration of the manufacturing variability of the input parameters, dimension ( $d$ ) and material properties ( $m$ ), calculated distribution of the buckling, computational error, and PTD of buckling load including the computational error**

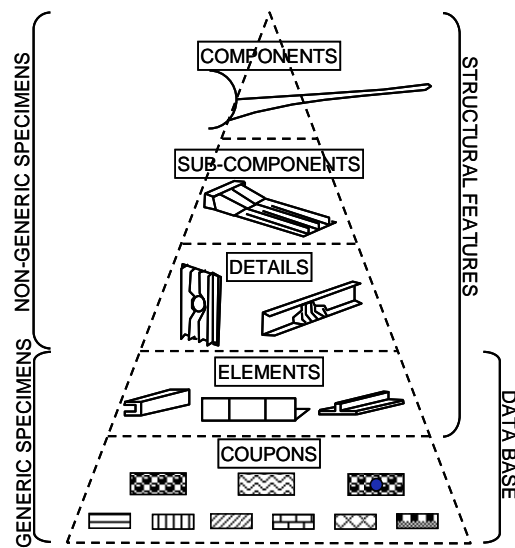


**Figure 2. Building-block approach for testing aircraft structural components.**

However considering every possible error may bring other concern that the calculated PF could be too conservative. Thus the error in the error bounds has to be reduced by structural tests. In the element test stage, the error in the computational model is reduced and we can reduce probability that the too conservative PF estimate.

Figure 4a shows an example that the PTD leads too conservative PF estimate. In this example, we estimate variability of buckling load  $\lambda$  of a panel design. Probability that the buckling load is less than the design allowable is the PF of design. The  $f_{true}(\lambda)$  is true capacity distribution of the panel which is unknown. The area on the left of the design allowable  $\lambda_{allow}$  is the true PF. On the other hand, the  $f_{calc}(\lambda)$  is the calculated distribution using the computational model. Due to the error in the computational model, the calculated PF has tremendous error, dangerously underestimate the PF. Figure 4b shows an example that the conservativeness in the PTD is effectively reduced by test.

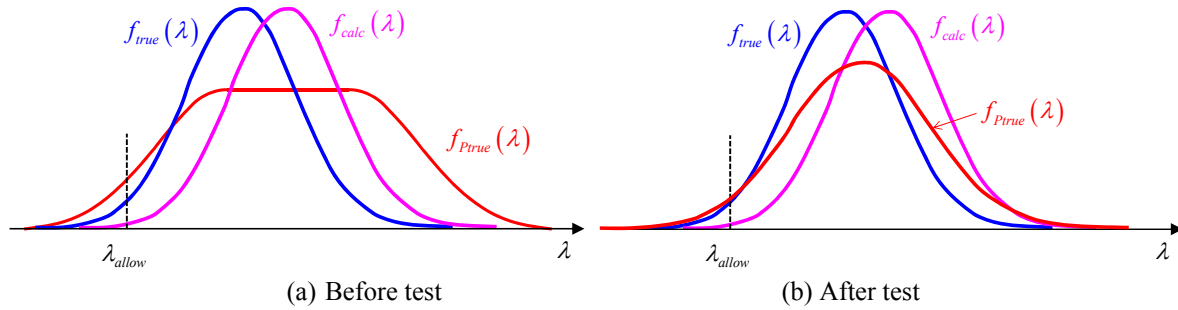


**Figure 4. Illustration of unconservative calculation of buckling load when including the error in the estimate improves the estimate of the PF**

Particularly for design with composite material, we should consider correlation between material properties due to the fiber volume fraction. Ignoring the correlation of the material properties induces error in predicting PF (Ref. 1). Also imperfection has a major source of variability in design capacity. Hilburger and Starnes (Ref. 7) investigated the effects of imperfections on the non-linear response and buckling loads of un-stiffened thin-walled compression-loaded graphite-epoxy cylindrical shells, they categorized imperfection types into two, traditional imperfection and non-traditional imperfection. The traditional Imperfection is considered into the uncertainty modeling. The effects of the imperfection for the curved panel example are shown in the illustrative example section. In case of composite material tests, input uncertainty is critical, such as material properties and thickness of thin panel, but there are very little measurement errors for measuring capacities, measuring load, in test (Ref. 2). To incorporate experiment results for calibrating FE model, input uncertainties have to be converted to output uncertainty for given inputs.

## B. Estimating Variabilities in Capacities with Test

Variability in capacity of structures has to be estimated based on uncertainty sources, such as material properties and geometries. True variability of the capacity can only be measured with an infinite number of structural tests, but it is not feasible. Computational models are alternatively used for making a reasonable prediction of the variability in capacity. However, structural tests have to be performed and incorporated into the computational model due to the prediction error in the computational model. We describe an uncertainty model for incorporating the structural tests into the computational model.

Unfortunately a single structural test provides information about just one failure mode. The curved panel test, we assume presence of two failure modes, buckling failure and strength failure. Buckling load and strength failure load can be called as load capacities and they are correlated each other. We can improve the buckling load prediction with the test result, but cannot improve the strength failure capacity with a test in which buckling failure observed.

Here we assume that we are estimating buckling load for given dimension  $d$  and material property  $m$ . Relation between true value and calculated value for buckling load is expressed as below

$$C_{true}^{\lambda} | (d, m) = (1 - e^{\lambda_{calc, true}}) \lambda_{calc} \quad (2)$$

where the  $C_{true}^\lambda |(d, m)$  is true capacity for given dimension and material property  $d$  and  $m$ , the  $\lambda_{calc}$  is calculated buckling load and the  $e_{calc,true}^\lambda$  is true error in buckling load capacity calculation, is unknown, we should estimate the error and obtain possible true value of the capacity, including uncertainties in estimation process.

A global measurement, such as the buckling load, can directly be updated by performing a test. But strength failure load should take indirect way to reduce uncertainty in the strain calculation. Excessive local strain triggers strength failure. Error in strain calculation at the spot where a strain gauge is attached may different from the spot where the excessive local strain actually appeared. An important assumption is made that measured strain, where the strain gauge is attached, at the buckling point can be compared to calculated strain at the same spot. Calculation error at the nearby spot can be used as strain calculation error for the other spots.

Here we propose a scheme to reduce uncertainty in the strength failure prediction with test result. We use failure theory to predict strength failure. The maximum strain theory is known as one of the best theory to predict strength failure of composite structures. Particularly for the strength failure capacity, we have two uncertainty sources that uncertainty in strain calculation and uncertainty in the failure theory itself. The former uncertainty is associated with the error in the computational model and the latter uncertainty is relevant to lacking knowledge.

If the computational model has no error, we only have the error in the failure theory as shown as

$$C_{true}^s |(d, m) = (1 + e_{true}^f) S_{true} \quad (3)$$

where the load  $S_{true}$  is the load when the maximum ply strain is equal to ultimate strain, and  $e_{true}^f$  is true error in the failure theory to have the true capacity for the strength failure. Actually our computational model evaluates the function between strain and load; i.e. a load-strain curve. If we have no error in our computational model to evaluate the curve, we can find the true load  $S_{true}$  for the ultimate strain as

$$S_{true} = f_{true}^s (\varepsilon_u) \quad (4)$$

The computational model brings error for both strain and load calculation. A reason we have to use two errors for both parameters is as follows. We can calculate the buckling load and corresponding strain from load-strain history. We have the history curve from the experiment. If we can express the history curve as a function of the buckling load and the corresponding strain, we can modify the calculated load-strain curve with those buckling load and the corresponding strain values and it provides us better prediction for the load  $S_{true}$  for given ultimate strain.

Figure 5 shows difference between the calculated load-strain curve and the true curve. In the curve, we have a relation between buckling load and strain, it implies that there is coupling between two variables.

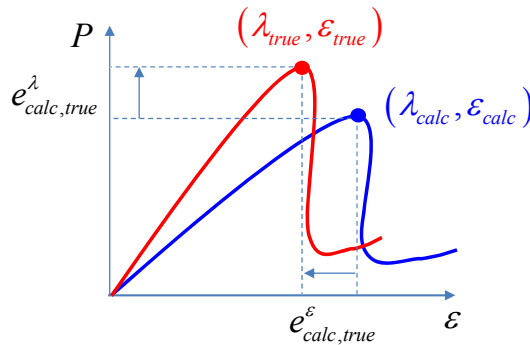


**Figure 5. Illustrations for errors in load-strain curve**

Since errors in buckling load calculation and strain calculation are also coupled. This is because as buckling approaches the nonlinear amplification of strains intensifies. Here we propose an approximation of the coupling between the two based on normalizing the curve, and fitting the normalized curve with Kriging surrogate model.

$$\frac{P}{\lambda_{calc} (1 - e^{\lambda_{calc,true}})} \approx \hat{f}_{KRG} \left( \frac{\varepsilon}{\varepsilon_{calc} (1 - e^{\varepsilon_{calc,true}})} \right) \quad (5)$$

where  $e^{\varepsilon_{calc,true}}$  is the true error in calculation of strain at buckling point,  $\hat{f}_{KRG}$  is Kriging model constructed based on the calculated load-strain curve. The Kriging model fits the experimental data for  $P$  and  $\varepsilon$ . Figure 5 shows that the discrepancies between the calculated load-strain curve and the true load-strain curve. When we know the true errors  $e^{\lambda_{calc,true}}$  and  $e^{\varepsilon_{calc,true}}$ , using Eq. (5), the true strength failure capacity for the ultimate strain  $\varepsilon_u$  is given as

$$S_{true} = \lambda_{calc} (1 - e^{\lambda_{calc,true}}) \hat{f}_{KRG} \left( \frac{\varepsilon_u}{\varepsilon_{calc} (1 - e^{\varepsilon_{calc,true}})} \right) \quad (6)$$

However the true errors are unknown, we have to estimate them. To discover the errors, structural tests are performed and the errors in calculation are calibrated. Before test, the errors are modeled as a uniform distribution, which is called as a prior distribution. Bounds of the uniform distribution represent estimated uncertainty in the computational model from experts. After test, using the Bayesian inference, we can update the initial distribution with test results. If there are no errors in tests and measurements, calculated values have pure theoretical errors. The test results are expressed as

$$\begin{aligned} \lambda_{true} &= \lambda_{calc} (1 - e^{\lambda_{calc,true}}) \\ \varepsilon_{true} &= \varepsilon_{calc} (1 - e^{\varepsilon_{calc,true}}) \end{aligned} \quad (7)$$

where  $\lambda_{true}$  and  $\varepsilon_{true}$  are the true buckling load and strain at the buckling load for given dimension and material property,  $d$  and  $m$ .  $\lambda_{calc}$  and  $\varepsilon_{calc}$  are calculated buckling load and strain using the computational model. Note that the errors are referred to the calculated values.

However the error distributions are conservative estimate to compensate possible error in the estimation. Including these errors for buckling load and surface strain can provide very conservative PF prediction as shown in Fig. 4a. The prior error distribution is denoted PTD and is expressed as follows

$$\begin{aligned} f_{e,\lambda}^{init} (e^{\varepsilon_{calc,Ptrue}}) &= \frac{1}{(u_e^\lambda - l_e^\lambda)} I(e^{\lambda_{calc,Ptrue}} \in [l_e^\lambda, u_e^\lambda]) \\ f_{e,\lambda}^{init} (e^{\varepsilon_{calc,Ptrue}}) &= \frac{1}{(u_e^\varepsilon - l_e^\varepsilon)} I(e^{\varepsilon_{calc,Ptrue}} \in [l_e^\varepsilon, u_e^\varepsilon]) \end{aligned} \quad (8)$$

where the  $I(x \in [l, u])$  is an indicator function that gives 1 for  $x$  belongs to the range  $[l, u]$  and 0 for otherwise, the  $u$  and  $l$  represent upper bound, and lower bound, respectively. The superscript  $\lambda$  and  $\varepsilon$  represent buckling load and strain, respectively.

After the test, we can reduce the error based on the test result. From the test, we can construct likelihood function of the responses. The form of the likelihood function is a function of likelihood of true prediction for the measured material property and dimensions of test specimen. For one structural test and its measured test results are  $\lambda_{meas}$  and  $\varepsilon_{meas}$  at dimension of  $d$  and material properties of  $m$  the effects of test errors is expressed as

$$\begin{aligned} \lambda_{true} &= \lambda_{meas} (1 - e^{\lambda_{test,true}}) \\ \varepsilon_{true} &= \varepsilon_{meas} (1 - e^{\varepsilon_{test,true}}) \end{aligned} \quad (9)$$

When substitute Eq. (9) into Eq. (7), it leads to

$$\begin{aligned}\lambda_{meas} (1 - e^{\lambda_{test,true}}) &= \lambda_{calc} (1 - e^{\lambda_{calc,true}}) \\ \varepsilon_{meas} (1 - e^{\varepsilon_{test,true}}) &= \varepsilon_{calc} (1 - e^{\varepsilon_{calc,true}})\end{aligned}\quad (10)$$

In the present model, we have two errors: error in simulation and error in test. In Eq. (10), true values of the errors in test are unknown. The errors are estimated and modeled as random variables as Eq. (11).

$$\begin{aligned}\hat{\lambda}_{Pmeas} &= \lambda_{meas} (1 - \hat{e}_{test,Ptrue}^{\lambda}) \\ \hat{\varepsilon}_{Pmeas} &= \varepsilon_{meas} (1 - \hat{e}_{test,Ptrue}^{\varepsilon})\end{aligned}\quad (11)$$

where  $\hat{e}_{test,Ptrue}^{\lambda}$  and  $\hat{e}_{test,Ptrue}^{\varepsilon}$  are random variables which follows estimated PDF of test error.  $\hat{\lambda}_{Pmeas}$  and  $\hat{\varepsilon}_{Pmeas}$  are used as the likelihood function, due to error in test in the Bayesian inference. Substituting the Eq. (11) into the LHS of the Eq. (10), we can obtain the calculation errors as

$$\begin{aligned}\hat{e}_{calc,Ptrue}^{\lambda} &= 1 - \frac{\hat{\lambda}_{Pmeas}}{\lambda_{calc}} \\ \hat{e}_{calc,Ptrue}^{\varepsilon} &= 1 - \frac{\hat{\varepsilon}_{Pmeas}}{\varepsilon_{calc}}\end{aligned}\quad (12)$$

where  $\hat{\lambda}_{Pmeas}$  and  $\hat{\varepsilon}_{Pmeas}$  are random variables which have possible true distribution for given  $d$  and  $m$  and they can be obtained after test. Detailed derivation is given in the next estimating errors in structural test section. From the Eq. (12), we can construct likelihood functions  $l_{e,\lambda}(e^{\lambda_{calc,Ptrue}})$  and  $l_{e,\varepsilon}(e^{\varepsilon_{calc,Ptrue}})$ .

Using the prior distribution in Eq. (8) and the likelihood functions, the distributions of errors in the response calculations are updated as

$$\begin{aligned}f_{e,\lambda}^{upd}(e^{\lambda_{calc,Ptrue}}) &= \frac{\int_{e^{\lambda}}^{e^{\lambda_{calc,Ptrue}}} f_{e,\lambda}^{init}(e^{\lambda_{calc,Ptrue}}) l_{e,\lambda}(e^{\lambda_{calc,Ptrue}}) de^{\lambda}}{\int_{e^{\lambda}}^{e^{\lambda_{calc,Ptrue}}} f_{e,\lambda}^{init}(e^{\lambda_{calc,Ptrue}}) l_{e,\lambda}(e^{\lambda_{calc,Ptrue}}) de^{\lambda}} \\ f_{e,\varepsilon}^{upd}(e^{\varepsilon_{calc,Ptrue}}) &= \frac{\int_{e^{\varepsilon}}^{e^{\varepsilon_{calc,Ptrue}}} f_{e,\varepsilon}^{init}(e^{\varepsilon_{calc,Ptrue}}) l_{e,\varepsilon}(e^{\varepsilon_{calc,Ptrue}}) de^{\varepsilon}}{\int_{e^{\varepsilon}}^{e^{\varepsilon_{calc,Ptrue}}} f_{e,\varepsilon}^{init}(e^{\varepsilon_{calc,Ptrue}}) l_{e,\varepsilon}(e^{\varepsilon_{calc,Ptrue}}) de^{\varepsilon}}\end{aligned}\quad (13)$$

Note that the errors in calculation for the buckling load and strain are correlated and modeled as joint PDF.

Finally, from Eq. (2), Eq. (3), Eq. (6) and estimated errors as shown in Eq. (8), error estimates before test, or Eq. (13), error estimates after test, the possible true capacities are obtained.

$$\begin{aligned}\hat{C}_{Ptrue}^{\lambda} \Big|_{d,m} &= (1 - \hat{e}_{calc,Ptrue}^{\varepsilon}) \lambda_{calc} \\ \hat{C}_{Ptrue}^s \Big|_{d,m} &= (1 - \hat{e}_{Ptrue}^f) \lambda_{calc} (1 - \hat{e}_{calc,Ptrue}^{\lambda}) \hat{f} \left( \frac{\varepsilon_u}{\varepsilon_{calc} (1 - \hat{e}_{calc,Ptrue}^{\varepsilon})} \right)\end{aligned}\quad (14)$$

where  $\hat{e}_{Ptrue}^f$  is follows uniform distribution with error bounds of failure theory.

### C. Estimating Likelihood Function of Structural Test

In structural test, there are measurement errors and errors in test conditions. Gage repeatability and reproducibility (GRR) is an important issue for structural test. For tests of composite panels, measurement errors in strain or buckling load are small, less than 0.1%, whereas measurement error in material properties and thickness are

relatively large, 3 to 4%. These errors are converted into errors in the buckling load and strain through the computational model.

In this section we describe how to obtain the errors in test. We estimate possible true buckling load and surface strain for the measured geometry and material property  $d_{meas}$  and  $m_{meas}$ . When we perform a test, dimension and material properties are measured as  $d_{meas}$  and  $m_{meas}$ . However the measurements are not necessarily be true values as shown in Fig. 6. But what we have in output is the true buckling load because measurement error in output is negligibly small. To compare the computational model with the test result, we should know a pair of measured inputs and true output because the measured buckling load is used to determine error in calculated buckling load with the measured inputs using a computational model. The true output is unknown, the true test error is the error between the measured buckling load and true buckling load.

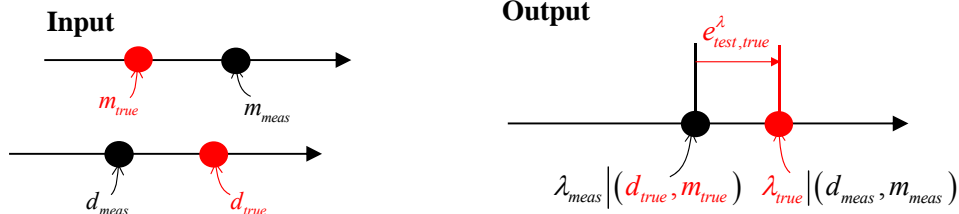


**Figure 6:** Illustrations for error in test due to input errors

Hence, the true bucklingload should be estimated using the measured inputs and possible true inputs. Left distributions represent input uncertainties in geometry  $d$  and material  $m$  property measurements. Figure 7 shows possible true input parameters and corresponding possible true buckling load. The possible true buckling load distribution represents possible true buckling loads for every possible true  $d$  and  $m$  for the measured  $d$  and  $m$ .

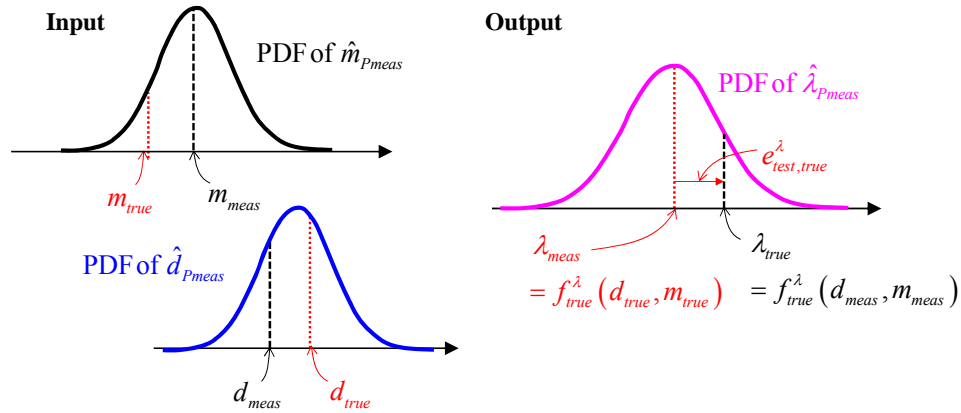


**Figure 7.** Illustrations for errors in inputs and corresponding errors in outputs when the measured  $d$  and  $m$  are true

From the Fig. 7, if we predict true buckling load and strain and we know variability in the inputs, we can calculate distributions for buckling load and strain according to the inputs uncertainty and we can express the distribution of possible true values with respect to the measured geometry and material property as

$$\begin{aligned}\hat{\lambda}_{est,Ptrue} &= f_{\lambda,true}(\hat{d}_{Pmeas}, \hat{m}_{Pmeas}) \\ \hat{\lambda}_{est,Ptrue} &= f_{\varepsilon,true}(\hat{d}_{Pmeas}, \hat{m}_{Pmeas})\end{aligned}\tag{15}$$

where bold  $d_{Pmeas}$  and  $m_{Pmeas}$  are random variables. The left values are the possible true buckling load and strain and they are random variables. If we use the computational model, the Eq. (15) can be rewritten as



$$\begin{aligned}
f_{\lambda,true}(\hat{d}_{Pmeas}, \hat{m}_{Pmeas}) &= \left(1 - e^{\lambda_{calc,true}}(\hat{d}_{Pmeas}, \hat{m}_{Pmeas})\right) f_{\lambda,calc}(\hat{d}_{Pmeas}, \hat{m}_{Pmeas}) \\
f_{\varepsilon,true}(\hat{d}_{Pmeas}, \hat{m}_{Pmeas}) &= \left(1 - e^{\varepsilon_{calc,true}}(\hat{d}_{Pmeas}, \hat{m}_{Pmeas})\right) f_{\varepsilon,calc}(\hat{d}_{Pmeas}, \hat{m}_{Pmeas})
\end{aligned} \tag{16}$$

The true errors,  $e^{\lambda_{calc,true}}$  and  $e^{\varepsilon_{calc,true}}$ , in calculations are functions of the dimensions and material properties generally. When their design and material properties are measured as  $d_{meas}$  and  $m_{meas}$  and variation in dimensions and material properties are small, it is assumed that the variation of error is also small. Eq. (16) can then be approximated as

$$\begin{aligned}
f_{\lambda,true}(\hat{d}_{Pmeas}, \hat{m}_{Pmeas}) &\approx \left(1 - e^{\lambda_{true}}(d_{meas}, m_{meas})\right) f_{\lambda,calc}(\hat{d}_{Pmeas}, \hat{m}_{Pmeas}) \\
f_{\varepsilon,true}(\hat{d}_{Pmeas}, \hat{m}_{Pmeas}) &\approx \left(1 - e^{\varepsilon_{true}}(d_{meas}, m_{meas})\right) f_{\varepsilon,calc}(\hat{d}_{Pmeas}, \hat{m}_{Pmeas})
\end{aligned} \tag{17}$$

If possible true errors for estimating the true error in test  $e^{\lambda_{test,true}}$  and  $e^{\varepsilon_{test,true}}$  are defined as

$$\begin{aligned}
1 - e^{\lambda_{test,true}} &= \frac{f_{true}^{\lambda}(d_{true}, m_{true})}{f_{true}^{\lambda}(d_{meas}, m_{meas})} \\
1 - e^{\varepsilon_{test,true}} &= \frac{f_{true}^{\varepsilon}(d_{true}, m_{true})}{f_{true}^{\varepsilon}(d_{meas}, m_{meas})}
\end{aligned} \tag{18}$$

By substituting Eq. (17) for the numerator of Eq. (18) due to measurement uncertainty and replacing the denominator of Eq. (18) using the true functions and true errors, we can obtain possible true values of buckling load and strain for the measured dimension and material property. Even we do not know the values of errors in calculations, with the constant error assumption in Eq. (17) with small variation, the possible true errors are calculated as

$$\begin{aligned}
1 - \hat{e}^{\lambda_{test,Ptrue}} &= \frac{f_{\lambda,calc}(\hat{d}_{Pmeas}, \hat{m}_{Pmeas})}{\lambda_{calc}} \\
1 - \hat{e}^{\varepsilon_{test,Ptrue}} &= \frac{f_{\varepsilon,calc}(\hat{d}_{Pmeas}, \hat{m}_{Pmeas})}{\varepsilon_{calc}}
\end{aligned} \tag{19}$$

Eq. (20) is obtained using Eq. (10) and Eq. (19), estimated calculation error after test will be expressed as

$$\begin{aligned}
\hat{e}^{\lambda_{calc,Ptrue}} &= 1 - \frac{f_{\lambda,calc}(\hat{d}_{Pmeas}, \hat{m}_{Pmeas}) \lambda_{test,meas}}{\lambda_{calc}^2} \\
\hat{e}^{\varepsilon_{calc,Ptrue}} &= 1 - \frac{f_{\varepsilon,calc}(\hat{d}_{Pmeas}, \hat{m}_{Pmeas}) \varepsilon_{test,meas}}{\varepsilon_{calc}^2}
\end{aligned} \tag{20}$$

PDFs of the possible true errors in Eq. (20) can be used for the likelihood function for the measured dimensions and material properties.

Here two scattered plots of the likelihood function are shown after test of the simple beam example in the illustrative example section. We have two associated values with the likelihood function: true error in buckling load and strain calculation and measured error in buckling load and strain calculation at the buckling load. The former values are obtained from true values with respect to the measured dimensions and material properties, showing true errors in calculations. The latter values are measured calculation errors values that including errors in test. Fig. 8 shows that an illustration of a scattered plot of the likelihood with 1000 samples and a set of true errors and a set of

measured errors. The horizontal axis is error in strain calculation and the vertical axis is error in buckling load calculation.

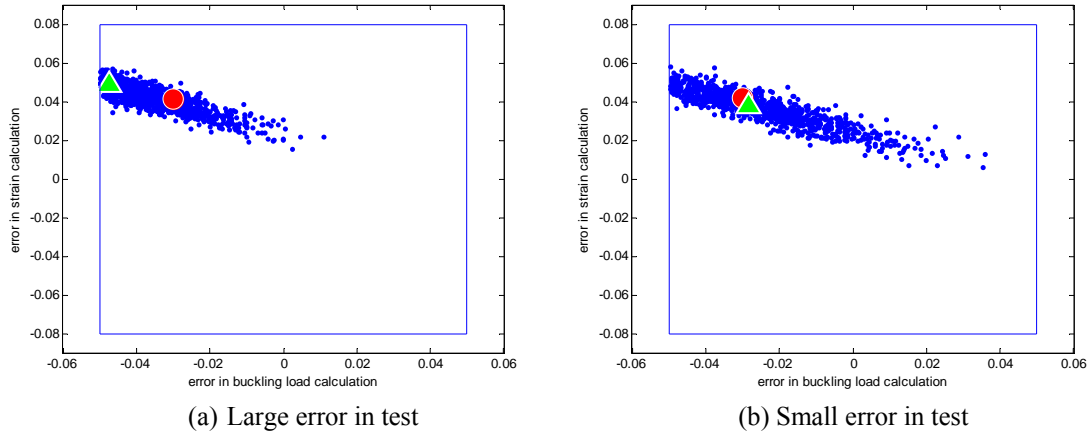


**Figure 8. A scattered plot of the likelihood function (1000 samples), true error (red circle) and measured error (green triangle)**

Note that the left plot does not include the measured error but the right plot does because measured errors are placing out of the prior, blue rectangle, the prior cut off the measured errors but still accommodate the true error.

#### D. Estimating Probability of Failure

In the previous sections, we make an uncertainty model of the composite structure capacities for given dimensions and material properties using the estimated likelihood function from a test. We can obtain the possible true capacities for certain measured dimensions and material properties of the test specimen. However, dimensions and material properties can vary due to uncertainty in manufacturing process. We assume that the error function from a single test can be used for other possible sets without applying extrapolation error since manufacturing variability is small.

The possible true capacities are obtained from combination between calculated variabilities of buckling load and strength failure load and the corresponding possible true calculation errors from an element test. We use MCS to evaluate the variability of the calculated buckling load and strength failure load and the possible true calculated error.

The composite panel requires a non-linear quasi-statics analysis to estimate buckling load and strain due to large deflection of the panel at the buckling point. Thus we have to consider load-strain history, which makes it hard to use a surrogate model. However, MCS requires high computational resources for very small PF, such as reliability index of  $\beta=4$  or 5. Hence, we use MCS for generating capacity samples of buckling load and strength failure load for uncertainty in dimensions and material properties and fit the samples using the goodness of fit tests to calculate the low level PFs. We extrapolate distributions of the capacities.

In order to calculate PF from Eq. (1), we have to consider critical failure mode. For given material property and dimension, we can predict buckling failure or strength failures. When we run simulations to obtain samples for  $\hat{C}_{Ptrue}^{\lambda}$  and  $\hat{C}_{Ptrue}^s$ , some simulations show that buckling failure is their critical failure mode and the others show strength failure mode is their critical failure mode. Therefore, Eq. (1) can be re-written as

$$Pf = \Pr\left(\hat{C}_{Ptrue}^{\lambda} \mid \left(\hat{C}_{Ptrue}^{\lambda} < \hat{C}_{Ptrue}^s\right) < \hat{P}\right)P_b + \Pr\left(\hat{C}_{Ptrue}^s \mid \left(\hat{C}_{Ptrue}^s < \hat{C}_{Ptrue}^{\lambda}\right) < \hat{P}\right)P_s \quad (21)$$

where  $P_b$  is probability that buckling failure mode is the critical failure mode, and  $P_s$  is probability that strength failure mode becomes the critical failure mode.

Due to the important feature of the independent random variables,  $\hat{C}_{Ptrue}^{\lambda} \mid \left(\hat{C}_{Ptrue}^{\lambda} < \hat{C}_{Ptrue}^s\right)$  and  $\hat{C}_{Ptrue}^s \mid \left(\hat{C}_{Ptrue}^s < \hat{C}_{Ptrue}^{\lambda}\right)$ , since one sample cannot have both capacities, we can gather samples which satisfying those conditions and fit two independent CDFs for each case, which are approximated distribution of those two random variables. Table 1 shows detailed process to calculate PF

**Table 1:** Probability of failure calculation process

<ol style="list-style-type: none"> <li>1. Generate <math>N</math> random sets of dimension <math>d</math> and material property <math>m</math> for their variability due to manufacturing process</li> <li>2. Calculate <math>N</math> capacities with respect to the generated <math>N</math> sets of <math>d</math> and <math>m</math> using an analysis code (If test is performed go to step 3, otherwise go to step 6)</li> <li>3. Generate <math>M</math> sample sets of <math>\hat{d}_{P_{meas}}</math> and <math>\hat{m}_{P_{meas}}</math> for possible variations due to measurement error</li> <li>4. Calculate <math>M</math> sample sets of <math>\hat{e}_{calc,Ptrue}^\lambda</math> and <math>\hat{e}_{calc,Ptrue}^\epsilon</math> using test results which presented in ref [0] and <math>f_{\lambda,calc}(\hat{d}_{P_{meas}}, \hat{m}_{P_{meas}})</math> and <math>f_{s,calc}(\hat{d}_{P_{meas}}, \hat{m}_{P_{meas}})</math> with respect to the generated <math>\hat{d}_{P_{meas}}</math> and <math>\hat{m}_{P_{meas}}</math> using the analysis code</li> <li>5. Fit the <math>M</math> sample sets of <math>\hat{e}_{calc,Ptrue}^\lambda</math> and <math>\hat{e}_{calc,Ptrue}^\epsilon</math> using copula and marginal PDFs. (go to step 7)</li> <li>6. Generate <math>M</math> errors using error bounds of buckling load and strain calculations</li> <li>7. Generate <math>Q</math> possible true errors in buckling load and strain using the fitted copula model</li> <li>8. Combine the <math>N</math> sets from the step 2 and <math>Q</math> samples from step 6 and obtain <math>N \times Q</math> samples capacities</li> <li>9. Separate those capacity samples into two failure cases of buckling failure and strength failure and fit those samples to two CDFs</li> <li>10. Generate a large number of <math>R</math> samples from the two CDFs and <math>R</math> samples from random design load distribution and calculate PF using Eq. (20)</li> </ol>
---

Note that K-S goodness to fit test is used for fitting the generated samples. Bayesian inference has strong point to identify the best fit CDF if the number of samples is small, the K-S test is affordable with enough number of samples.

### III. Illustrative Examples

In this section, we show a simple numerical example to validate the uncertainty model in the first place and estimating PF, followed by composite panel example

#### A. Composite Beam Example

The present study is intended to validate the uncertainty model. Here we have a simple composite beam model with two potential failure modes, buckling failure and strength failure, and a single element test is performed and buckling failure mode observed in the test. In this example, we simulate testing and estimating process. We make two equation types for buckling load and strength failure load: true equations and theoretical equations. The true equation give true buckling load and strain but the theoretical equations have errors in their predictions. We estimate PF using the theoretical equations and incorporate the test result made by the true equations. The test gives measured buckling load, strain at the buckling point, material properties and dimensions. The measured material properties and dimensions have measurement errors. Since we know the true equations, not like reality, the estimated PF will be verified to true PF calculated by the true equations. To see the effects of test variability and MCS error, we repeat the process 1000 times.

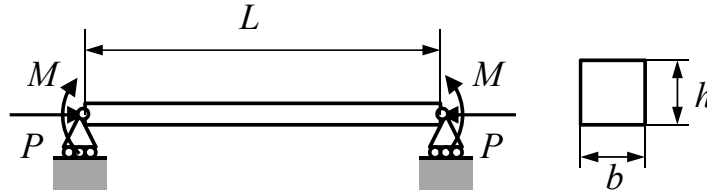


**Figure 9.** Simple beam model

Dimensions and boundary conditions are shown in the Fig. 9. We have bending moments  $M$  and axial forces  $P$  with roller boundary conditions on both sides. The bending moment  $M$  is deterministic and the axial load  $P$  has uncertainty. Hence PF of the structure is a function of the axial force  $P$  for given  $M$ . Theoretical equations for calculated buckling load  $P_{calc}^\lambda$  and strength failure load  $P_{calc}^s$  and corresponding true values  $P_{true}^\lambda$  and  $P_{true}^s$  are expressed in Table 2.

**Table 2:** Theoretical equation and true equation

	Buckling load	Strength failure load
Theoretical equation	$P_{calc}^\lambda = \frac{\pi^2 EI}{l^2} - \frac{M^2}{4EI}$	$ \varepsilon_{calc}  \leq \varepsilon_u$ $\varepsilon_{calc} = -\left(\frac{P_{calc}^s}{EA} + \frac{0.5hM}{EI}\right)$
True equation	$P_{true}^\lambda = 0.97\left(\frac{\pi^2 EI}{l^2} - \frac{M^2}{4EI}\right)$	$1.02 \varepsilon_{true}  \leq \varepsilon_u$ $\varepsilon_{true} = -1.05\left(\frac{P_{true}^s}{EA} + \frac{0.5hM}{EI}\right)$

PF estimation process in Table 1 is used. Test is performed as follows:

- 1) Generate a test result of buckling load and strain at the buckling point (buckling failure)
- 2) Generate measured dimensions and material properties by adding measurement uncertainty on the true dimensions and material properties

We have two examples to consider different failure mode patterns: multiple failure modes with and without failure mode switching. Dominant failure mode is buckling failure mode for both examples. Example 1 has no failure mode switching and example 2 has failure mode switching.

### 1. Composite Beam Example: no failure mode switching case

Firstly, we consider a structure with only an axial force case. Table 3 shows that an uncertainty list for material properties and dimensions.

**Table 3. Nominal values and variabilities from uncertainty sources**

Uncertainty source	Nominal value	Variability	Distribution
Manufacturing process	$E$ : 200 GPa $\varepsilon_u$ : 0.0025	CV=3% for $E$ CV=1% for $\varepsilon_u$	Normal
Measurement error	$E$ : 0% $\varepsilon_u$ : 0%	Std. of 1% for $E$ No error for $\varepsilon_u$	Normal
Manufacturing process	$b$ : 0.3 m $h$ : 0.165 m	$\pm 1\%$ for $b$ and $h$	Uniform
Measurement Error	$b$ : 0% $h$ : 0%	Std. of 0.5% for $b$ and $h$	Normal

The bending moment  $M=0$ , PF is estimated in terms of nominal  $P$ . We use table 1 to estimate PF, the number of function evaluations to obtain samples for capacities is  $N=200$ . For after test case, further function evaluations are needed to obtain samples for errors in calculations,  $M=100$ . Finally we have  $Q=100 \times N$  possible true capacity samples, separated into two cases,  $\hat{C}_{Ptrue}^\lambda | (\hat{C}_{Ptrue}^\lambda < \hat{C}_{Ptrue}^s)$  and  $\hat{C}_{Ptrue}^s | (\hat{C}_{Ptrue}^s < \hat{C}_{Ptrue}^\lambda)$ , fitted to CDFs.  $R=10$  Million are the number of sample generations from fitted CDFs and a CDF for load  $P$ .

Error bounds for errors in buckling load calculation, strain calculation and failure theory are given in Table 4.

**Table 4:** Error bounds

Error types	Error bounds
Error in buckling load calculation $e_{calc, Ptrue}^\lambda$	[-0.05, 0.05]
Error in strain calculation $e_{calc, Ptrue}^\varepsilon$	[-0.08, 0.08]
Error in failure theory $e_{Ptrue}^f$	[-0.05, 0.05]

We have the uncertainties due to the MCS and test variability, PF estimation process is repeated 1000 times. Statistics are compared to the true PF as table 5.

From the table 5, we can see the effects of test. We have a single test result to reduce uncertainty in calculations. We expect PF of  $2.61 \times 10^{-4}$  before test, whereas PF  $1.18 \times 10^{-4}$  after test for  $P=19$  MN. The effects of test for reducing uncertainty in predicting PF is significant. The difference will induce design weight reduction. The standard deviation PF without test represents error in MCS. We can observe that the standard deviation PF with test becomes

larger than the standard deviation PF without test. The portion comes from test variability. It is observed that test can significantly reduce conservativeness in the PF estimate, but also it adds one more variability source, standard deviation of the PF estimation increases.

**Table 5:** PF estimations with 1000 repetitions

Magnitude of $P$	19 MN	19.5 MN	20 MN
Mean PF	$1.18 \times 10^{-4}$	$5.91 \times 10^{-4}$	$2.42 \times 10^{-3}$
Std. PF	$5.85 \times 10^{-5}$	$2.27 \times 10^{-4}$	$7.34 \times 10^{-4}$
COV	0.5	0.38	0.3
Mean PF	$2.61 \times 10^{-4}$	$1.01 \times 10^{-3}$	$3.22 \times 10^{-3}$
Std. PF	$5.24 \times 10^{-5}$	$1.73 \times 10^{-4}$	$4.65 \times 10^{-4}$
COV	0.2	0.17	0.14
True PF	$4.68 \times 10^{-5}$	$2.96 \times 10^{-4}$	$1.42 \times 10^{-3}$
True PF (buckling failure)	$4.32 \times 10^{-5}$ (0.83) <sup>a</sup>	$2.68 \times 10^{-4}$ (0.83)	$1.30 \times 10^{-3}$ (0.81)
True PF (strength failure)	$1.86 \times 10^{-5}$ (0.17) <sup>b</sup>	$1.35 \times 10^{-4}$ (0.17)	$0.7 \times 10^{-4}$ (0.19)

<sup>a</sup> Probability of buckling failure

<sup>b</sup> Probability of strength failure

Secondly, we consider a structure with an axial force and a bending moment case. The structure has failure mode switching. In this example differences are the nominal value is  $h = 0.08$  m and bending moment  $M=105$  kN-m. PF is estimated in terms of nominal  $P$ . We use table 1 to estimate PF. The number of function evaluations is  $N=200$ . For after test case,  $M=100$  is used.  $Q=100 \times N$  and  $R=10$  Million. Error bounds are the same with the previous no bending moment example. PF estimation process is repeated 1000 times. Statistics are compared to the true PF as table 6.

**Table 6:** PF estimations with 1000 repetitions

Nominal $P$	2.1 MN	2.2 MN	2.3 MN
Mean PF	$1.72 \times 10^{-4}$	$5.72 \times 10^{-4}$	$3.24 \times 10^{-3}$
Std. PF	$1.44 \times 10^{-4}$	$3.97 \times 10^{-4}$	$1.62 \times 10^{-3}$
COV	0.84	0.69	0.5
Mean PF	$1.97 \times 10^{-3}$	$3.17 \times 10^{-3}$	$6.00 \times 10^{-3}$
Std. PF	$3.81 \times 10^{-4}$	$5.84 \times 10^{-4}$	$1.01 \times 10^{-3}$
COV	0.19	0.18	0.17
True PF	$8.8 \times 10^{-5}$	$3.63 \times 10^{-4}$	$2.54 \times 10^{-3}$
True PF (buckling failure)	$4.8 \times 10^{-6}$ (0.03) <sup>a</sup>	$1.45 \times 10^{-4}$ (0.33)	$2.19 \times 10^{-3}$ (0.80)
True PF (strength failure)	$8.6 \times 10^{-5}$ (0.97) <sup>b</sup>	$2.51 \times 10^{-4}$ (0.67)	$6.0 \times 10^{-4}$ (0.20)

<sup>a</sup> Probability of buckling failure

<sup>b</sup> Probability of strength failure

A notable thing is the ratio of the true PF for a single failure mode. For example, the ratio of buckling failure is 0.80 and the ratio for strength failure mode is 0.20 when nominal  $P$  is 2.3 MN. It implies that we can usually observe buckling failure modes from test. However, at low PF level, strength failure mode is dominant failure mode. For structures, this undetected failure mode by tests can bring a dangerous situation.

The PF without test provides very conservative estimate of PF because uncertainties in strain calculation and failure theory are combined. Error in strain calculation of 8% and error in failure theory of 2% are used in this simulation. So, the error in strain calculation is major uncertainty source to predict strength failure. After test, we can reduce the uncertainty in strain calculation, we can reduce uncertainty in strain calculation. Test result can effectively reduce conservativeness in the PF estimate without test.

## B. Curved Composite Laminated Panel with a Hole

In this section we describe PF estimation of the curved composite panel. FE model and analysis scheme of the panel is shown at the first place. We then discuss about uncertainty model of the composite panel. PF of this panel is estimated in terms of the axial force  $P$ .

### 1. Nonlinear Buckling analysis with ABAQUS

For analysis of this model, we use nonlinear analysis to predict strength failure and buckling failure as severe deflection is anticipated in the panel surface, especially around the hole boundary,

ABAQUS is used for the nonlinear analysis of the composite panel. The Riks method was used to trace incrementally the load-displacement curve and obtain buckling load. After the analysis processes, we track the load-displacement curve to figure out buckling point and obtain load at the point as buckling load. Also load-ply strain curves are analyzed on the nodes around the hole to find strength failure load.

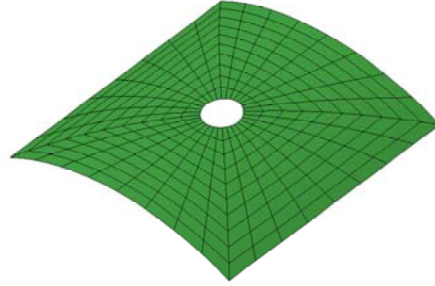


**Figure 10. Curved composite laminate panel modeling with ABAQUS**

The composite panel in Fig. 10 is modeled using ABAQUS with 9 node S9R5 element. The panel section is defined as composite general section property with stacking sequence and thickness as shown in Table 7.

**Table 7. Ply material properties / Ply section properties**

$E_1$	135 GPa (19600 ksi)	$\epsilon_{1tu}$	0.0093
$E_2$	13.0 GPa (1890 ksi)	$\epsilon_{1cu}$	-0.011
$G_{12},$ $G_{13}$	6.4 GPa (930 ksi)	$\epsilon_{2tu}$	0.0043
$G_{23}$	$E_2/3$	$\epsilon_{2cu}$	-0.016
$\nu_{12}$	0.38	$\epsilon_{12u}$	0.019
Ply thickness		0.142 mm (0.0056 inch)	
Stacking sequences		$[\pm 45/90/0_2/90/\mp 45]_s$	

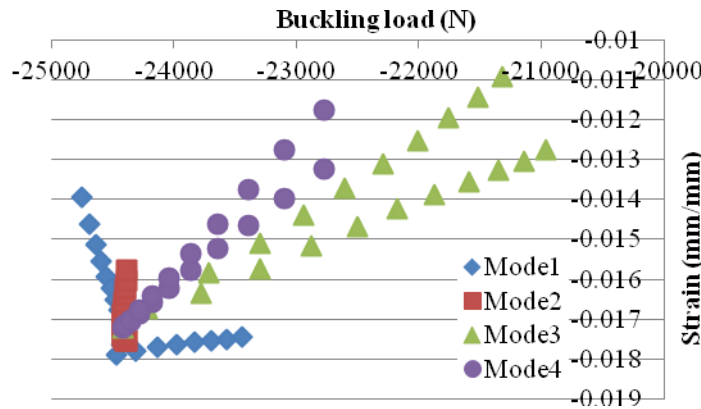


**Figure 11: Effects of various imperfections (estimated simulation error)**

We assume that ABAQUS is capable of providing accurate prediction. In this composite laminate panel, imperfection is very sensitive to buckling load prediction but the test specimen's imperfection data is not available. We assume that the imperfection which gives the best prediction is actual imperfection of the specimen. Figure 11 shows the effects of the imperfections with various perturbation magnitudes. -10% to 10% of thickness perturbations are assumed as reasonable imperfections and this represents imperfection in the panel. Mode 1 to 4 are used, eigenvector of the model 1 to 4 are shown in Appendix B. The eigenvector is obtained from the linear buckling analysis and the normal direction is surface normal direction of the curved panel. Actual test with the curved panel was performed by Knight (Ref. 3). Simulation result indicates that -10% thickness perturbation with mode 3

eigenvector provides the best predictions for buckling load and surface strain. Hence we assume that the specimen's actual imperfection is approximately mode 3 eigenvector shaped thickness perturbation of -10%. Figure 11 shows another fact that the effects of imperfection on buckling load and strain are very substantial.

Figure 12 shows comparisons between predicted load-displacement curve and load-surface strain curve from ABAQUS and corresponding test results. The curves are plotted up to buckling point. The surface strain is measured from two strain gages on the top and bottom of the panel near the hole. Table 8 has measured buckling load and surface strain at the buckling point from the test.

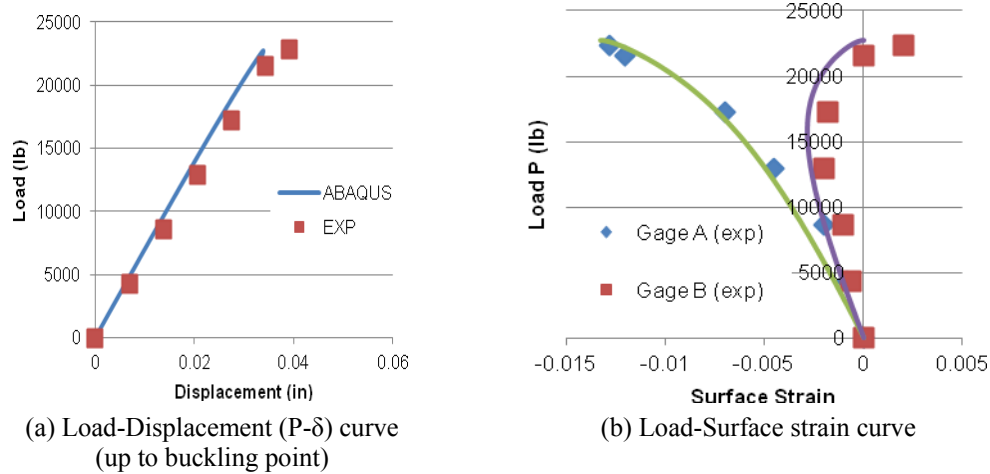


**Figure 12. Curved composite laminate panel modeling with ABAQUS**

**Table 8. Experiment results**

Buckling load	101.6 kN (22840 lb)
Surface strain	-0.0128

## 2. Uncertainty Modeling of Curved Composite Panel

In this section, variabilities in buckling load and strength failure load, capacities of the curved composite panel for the two failure modes, are estimated using ABAQUS. The two capabilities are varied due to variabilities in manufacturing process, such as material properties and geometric properties.

**Table 9: Variability of material properties, thickness, imperfection and load**

	Variabilities	Modeling
Material properties	CV=4.25% for $E_1$ , 2.75% for $E_2$ , 1.5% for $G_{12}$ and 5.25% for $\nu_{12}$ (correlated) CV=6% for $\epsilon_{1u}$ , and $\epsilon_{1l}$ , 10% for $\epsilon_{2l}$ , $\epsilon_{2u}$ and $\epsilon_{12u}$ * (independent)	Considering correlation between the parameters using Gaussian copula
Thickness	$\pm 3\%$ of thickness ( $0.0056 \times 0.03 = 0.00269$ in)	Uniform distribution for individual ply thickness
Imperfection	$\pm 10\%$ of thickness ( $0.0056 \times 16 \times 0.1 = 0.00896$ in)	Uniform distribution Imperfection mode is randomly selected among mode 1, 2, 3, and 4
Load	CV=10% for $P$	Normal distribution

Table 9 shows variabilities in material properties and geometries. In this table, ply material properties,  $E_1$ ,  $E_2$ ,  $G_{12}$  and  $\nu_{12}$ , are correlated. It is assumed that the fiber volume fraction is the dominant factor to make the correlation. Use relationships for the elastic constants in terms of volume fraction from mixture rule, the correlation between material properties are calculated. Variabilities of material properties are given in table 9. We assume that the nominal material properties in table 7 have variabilities in table 9 then covariance matrix is calculated. See detailed information in (Ref. 1). Also it is assumed that the ultimate strains are independent each other.

The others, thickness and imperfection are also shown here. It is assumed that all the plies have the same variability in thickness. For the variability in imperfection, we randomly select an eigenvector and multiply the perturbation factor which is generated from the uniform distribution.

Variabilities of capacities are estimated using the uncertainty sources and ABAQUS model with MCS. We predict the strength failure using load-strain curve from the FE analysis using the maximum strain criterion. Strength failure beyond the buckling point is estimated using post buckling analysis. 200 samples are generated using ABAQUS.

As we have error in measurements of dimensions and material properties, we need to consider test error Table 10 shows the uncertainty sources of test which cause the test error.

**Table 10: Uncertainty sources in structural test**

	Causes	Experimental variability	Modeling
Material properties <sup>1</sup>	Measurement	CV=1% for $E_1$ , 3% for $E_2$ , $G_{12}$ and $\nu_{12}$	Independent normal distributions
Thickness <sup>2</sup>	Measurement	$\pm 0.08\%$ of thickness (panel thickness: $0.0056 \times 16 = 0.0896$ in)	Uniform distribution
Imperfection <sup>3</sup>	Measurement	$\pm 0.08\%$ of thickness	Uniform distribution
Boundary <sup>4</sup> condition	Imperfect BC	Torsional springs on nodes applying BC	Ignored as for little effect
Load	Measurement	0.256 lb (experimental buckling load: 22840 lb)	Ignored as for little effect

Since these errors are correlated, the errors are modeled using Frank copula. Marginal distributions are fitted using K-S test to find the best fit CDFs. To fit the marginal distributions and copula, 200 samples are generated using ABAQUS with the uncertainty sources in structural test.

**Table 11: Uncertainty sources on experiment**

(200 samples)	Buckling load	Surface strain
Mean	22801.01	0.0132
Standard deviation	214.07	0.000063
COV (std. of error)	0.93%	0.47%
Kendal's tau	0.15	

Using Eq. (19), we obtain distribution of  $1 - \hat{e}_{test, Ptrue}^\lambda$  and  $1 - \hat{e}_{test, Ptrue}^\epsilon$ , scattered plot and fitted joint PDF of likelihood function are shown in Fig. 13 and table 12 shows marginal CDFs for each calculation errors. Rank correlation coefficient Kendal's tau of the likelihood function is 0.15.

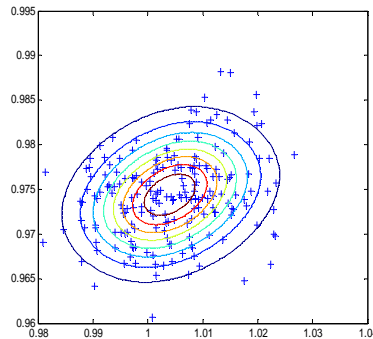


**Figure 13: Updated 1-e distribution for both buckling and strain (200 FE analysis runs)**



Same error bounds as shown in table 4 are used for establishing prior distribution, updated distribution of the calculation errors are used to estimate PF.

**Table 12:** K-S test to identify the best fit CDF for buckling load and surface strain

	Error in buckling load	Error in surface strain
CDF type	Logn	Gamma
Mean	1.0041	0.975
Standard deviation	0.0094	0.0046
COV (std. of error)	0.93%	0.47%
Kendal's tau	0.15	

### 3. Estimating Probability of Failure Based on a Single Test

PFs and their corresponding reliability indices of the composite panel are estimated in terms of loads. As expected the effects of test is significant in terms of PF.

**Table 13:** Estimated PFs according to load P

Load P (kN)	After test			Before test		
	PF	$\beta$	Dominancy	PF	$\beta$	Dominancy
80	$4.6 \times 10^{-3}$	2.61	0.73 (B)	$7.8 \times 10^{-3}$	2.42	0.57 (B)
77.5	$1.7 \times 10^{-3}$	2.92	0.74 (B)	$3.3 \times 10^{-3}$	2.71	0.56 (B)
75	$5.7 \times 10^{-4}$	3.25	0.73 (B)	$1.3 \times 10^{-3}$	3.01	0.56 (B)
72.5	$1.6 \times 10^{-4}$	3.59	0.73 (B)	$4.4 \times 10^{-4}$	3.33	0.55 (B)
70	$4.2 \times 10^{-5}$	3.93	0.71 (B)	$1.2 \times 10^{-4}$	3.65	0.56 (B)

As we got from the previous examples, test affects a lot on PF estimate. With the test, we can significantly reduce conservativeness in the PF estimate before test. In the table we have dominancy ratios and the values represent probability of occurrence at the corresponding load. In this table the ratios shows that there is little chance of failure mode switching and buckling mode is a dominant failure mode of the curved composite panel.

## IV. Concluding Remarks

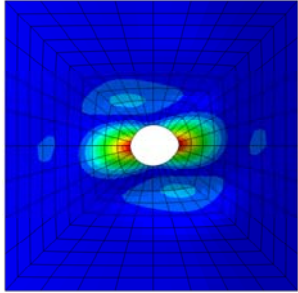
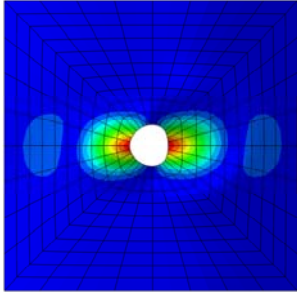
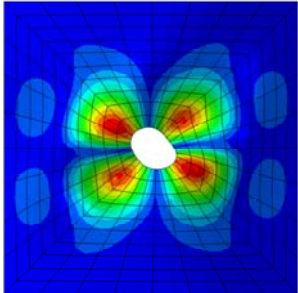
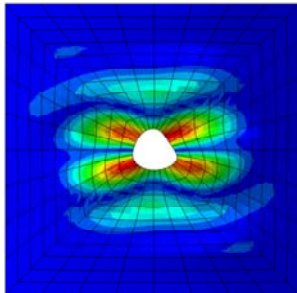
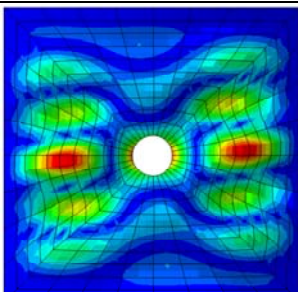
Advanced composite materials have become key ingredients in modern aircraft structures. We make an uncertainty quantification model for a curved composite fuselage panel. Both epistemic uncertainty and aleatory uncertainty are applied in the model. Two correlated failure modes, buckling failure and strength failure, are considered.

Through the uncertainty quantification model, we estimate PF of a structure. The PF estimation capability of the model is validated with a simple example. Also the effects of test are quantified in terms of PF. The numerical example shows that performing a single test can reduce significant conservativeness in PF estimation. Performing a single test for given probability of failure allows lighter structure. For the curved composite panel, ABAQUS is used for non-linear analysis to predict failures. PF of the curved panel according to the load level is estimated based on the analysis result with the uncertainty quantification method. Also probability of failure occurrence for each failure modes is estimated to see if there is a failure mode switching.

## Appendix

ABAQUS linear buckling analysis provides eigenvectors. The eigenvectors were used for the geometric imperfection.

**Table A1:** Normalized eigenvector contours

n=1	Description	n=4	Description
	Maximum magnitude of displacement: 1.073 (Mode1)		Maximum magnitude of displacement: 1.071 (Mode2)
	Maximum magnitude of displacement: 1.057 (Mode3)		Maximum magnitude of displacement: 1.081 (Mode4)
	Maximum magnitude of displacement: 1.022 (Mode5)		

## Acknowledgments

Authors would like to thank the National Science Foundation for supporting this work under the grants CMMI-0856431.

## References

<sup>1</sup>Smarslok, B. P., Haftka, R. T., and Ifju, P., “A Correlation Model for Graphite/Epoxy Properties for Propagating Uncertainty to Strain Response,” 23<sup>rd</sup> Annual Technical Conference of the American Society for Composites, Memphis, Tenn, 2008.

<sup>2</sup>Smarslok, B., Speriato, L., Schulz, W., Haftka, R. T., Ifju, P., Johnson, T. F., “Experimental uncertainty in Temperature Dependent Material Properties of Composite Laminates,” Society for Experimental Mechanics Annual Conference, No. 241, St. Louis, MO, June, 2006.

<sup>3</sup>Kight, N. F., and Starnes, J. H., “Postbuckling Behavior of Axially Compressed Graphite-Epoxy Cylindrical Panels With Circular Holes,” *Journal of Pressure Vessel Technology* 107: 394-402, 1985.

<sup>4</sup>Stanley, G. M., *Continuum-Based Shell Elements*, Ph.D. Dissertation, Department of Mechanical Engineering, Stanford University, 1985.

<sup>5</sup>Park, C., Matsumura, T., Haftka, R.T., Kim, N.H., and Acar, E., “Modeling the Effect of Structural Tests on Uncertainty in Estimated Failure Stress,” 13th AIAA/ISSMO/ Multidisciplinary Analysis and Optimization Conference, September 13-15, 2010, Fort Worth, Texas

<sup>6</sup>Acar, E., Haftka, R.T., and Kim, N.H., “Effects of Structural Tests on Aircraft Safety ” *AIAA Journal* ,Vol. 48(10), 2235–2248, 2010.

<sup>7</sup>M. W. Hilburger and J. H. Starnes Jr., “Effects of imperfections on the buckling response of compression-loaded composite shells,” *International Journal of Non-Linear Mechanics* 37 (2007) 623-643.

<sup>8</sup>Qu, X., Haftka, R.T., Venkataraman, S., and Johnson, T.F., “Deterministic and Reliability-Based Optimization of Composite Laminates for Cryogenic Environments,” *AIAA Journal*, 41(10), pp. 2029-2036, 2003.

<sup>9</sup>Villanueva, D., Haftka, R.T., Sankar, B.V. (2011) “ Including the Effect of a Future Test and Redesign in Reliability Calculations“ *AIAA Journal* ,Vol. 49(12), 2225–2230

<sup>10</sup>Noh, Y., K. K. Choi, Lee, I., (2010) “ Identification of marginal and joint CDFs using Bayesian method for RBDO“ *Journal of Structural Multidisciplinary Optimization* , Vol. 40, 35-51